PERGAMON

International Journal of Heat and Mass Transfer 42 (1999) 1305–1315

International Journal of HEAT and MASS TRANSFER

A two-equation turbulence model and its application to a buoyant diffusion flame

Zhenghua Yan*, Göran Holmstedt

Department of Fire Safety Engineering, Lund University, Box 118, S-22100 Lund, Sweden

Received 29 August 1997; in final form 3 July 1998

Abstract

A modified k–ε two-equation turbulence model was developed to improve the consideration of the important buoyancy effect on turbulence and turbulent transport, which is a serious deficiency of the standard buoyancy-modified k–ε model. The present model was tested against both plane and axisymmetric thermal plumes and a buoyant diffusion flame. The model was found to be stable, computationally economic, promising and applicable to complex situations. The predicted plume spreading rates and velocity and temperature profiles agreed well with experimental measurements. When compared with the standard buoyancy-modified k–ε turbulence model, this model gives significantly improved numerical results. © 1998 Published by Elsevier Science Ltd. All rights reserved.

Nomenclature

a_{gi} gravity acceleration vector
c_1, c_2 turbulence model constants
c_3 turbulence model constant
$c_{1\varepsilon}$, $c_{2\varepsilon}$ turbulence model constants
$c_{3\varepsilon}$, c_g turbulence model constants
c_{1t}, c_{2t} turbulence model constants
c_{3t} turbulence model constant
c_μ turbulence model constant
f mixture fraction
F_0 the buoyancy parameter
g mixture fraction variance
G buoyancy production rate of turbulence kinetic energy
I radiation intensity
k turbulence kinetic energy
l distance of a radiating path
P shear production rate of turbulence kinetic energy
P_r Prandtl number
r radial distance
R turbulence model constant
R_f flux Richardson number
R_f' modified flux Richardson number
s stoichiometric ratio
S_c Schmidt number
t time
T temperature
u_i, u_j velocity vector
v vertical velocity
z height above virtual origin of plume.

Greek symbols
β thermal expansion coefficient
δ_{ij} Kronecker delta
ε dissipation rate of turbulence kinetic energy
μ laminar viscosity
υ_t turbulent viscosity
ρ density
σ_k, σ_T turbulent Prandtl numbers
σ_ε, σ_φ turbulent Prandtl numbers
$\zeta_{w,l}$ local spectral absorption coefficient.

Subscripts
F fuel
i co-ordinate direction
m maximum
O oxidant
w wavenumber
∞ ambient condition.

* Corresponding author.

0017–9310/98/$ - see front matter © 1998 Published by Elsevier Science Ltd. All rights reserved.
PII: S001–7931(09)80020–63

Superscripts
— Reynolds average
~ Favre average
′ fluctuation from Reynolds average
″ fluctuation from Favre average.

1. Introduction

Buoyancy-affected flow is of great interest in many industrial applications, including fires and pollutant dispersion. In fires, the flow is usually buoyancy-dominated with a Froude number below 1.0. Among the complex processes involved in fires, buoyancy-affected turbulent transport is of great importance, since it imposes a direct and critical influence on entrainment, fire plume width, rate of descent of ceiling smoke layer, gas temperature and velocity profiles, and combustion, etc. Therefore, the accuracy of numerical simulation of fires is largely dependent on how well the buoyancy-affected turbulent transport is considered.

Due to its complexity, turbulence remains an unresolved subject of research. In order to meet engineering needs, many different turbulence models, of varying complexity and applicability have been proposed [1], such as the mixing length model, the k–ε model, the k–ω model, the Algebraic Stress Model (ASM) and the Reynolds Stress Model (RSM). With the rapid expansion of computer power, the Large Eddy Simulation (LES) and the Direct Numerical Simulation (DNS) have started to play an important role in fluid dynamics research. However, due to the enormous computer resources required, the LES and the DNS are still essentially impractical, especially for complex problems and industrial applications.

Among the turbulence models mentioned above, the k–ε turbulence model is perhaps the most widely used. Most fire simulations have been carried out using the k–ε turbulence model [2–8]. It is attractive because it is simple, numerically stable, extensively validated and requires much less computing capacity than the RSM and ASM. However, the standard buoyancy-modified k–ε model tends to seriously under-predict the spreading rate of vertical thermal plume [5, 6] and over-predict the spreading rate of horizontal, stably-stratified flow [9]. Shabbir and Taulbee [10] evaluated the closure formulations in the k–ε model and the ASM using experimental data. They found that the rate of turbulence kinetic energy production directly by buoyancy in an axisymmetric thermal plume is generally several times larger than that modeled through the simple gradient method in the standard buoyancy-modified k–ε model. Clearly, the consideration of the buoyancy effect in the standard buoyancy-modified k–ε model is far from adequate.

With a partial differential or algebraic equation solved for each individual Reynolds stress, the RSM and the ASM are able to account for the buoyancy effect much more realistically. In [10], it was found that the measured buoyancy production rate of turbulence kinetic energy agreed reasonably well with that evaluated in the ASM, which has been demonstrated to be quite successful, especially when applied to relatively simple fluid dynamics problems, such as a two-dimensional thermal plume and a two-dimensional jet. However, these two models, especially the RSM, are much more computationally demanding than the k–ε model, and numerically unstable [11, 12]. The numerical difficulty may become even worse when they are applied to more complex situations, such as those in fires in which combustion and radiation are involved.

It is clearly desirable to develop a relatively simple and k–ε based turbulence model which improves the consideration of the buoyancy effect significantly and allows the k–ε based CFD codes, which are being extensively used, to be easily modified. In this study, a modified k–ε two-equation turbulence model was developed. It was applied to both two-dimensional plane and axisymmetric thermal plumes as a basic test, and to a buoyant diffusion flame to demonstrate its applicability to complex situations.

2. Model development

In the standard buoyancy-modified k–ε model, turbulence is considered through the solution of the following two equations [13]:

$$\frac{\partial(\bar{\rho}k)}{\partial t}+\frac{\partial(\bar{\rho}\tilde{u}_j k)}{\partial x_j}=\frac{\partial}{\partial x_j}\left(\frac{\mu_t}{\sigma_k}\frac{\partial k}{\partial x_j}\right)+\bar{\rho}(P+G-\varepsilon) \tag{1}$$

$$\frac{\partial(\bar{\rho}\varepsilon)}{\partial t}+\frac{\partial(\bar{\rho}\tilde{u}_j \varepsilon)}{\partial x_j}=\frac{\partial}{\partial x_j}\left(\frac{\mu_t}{\sigma_\varepsilon}\frac{\partial \varepsilon}{\partial x_j}\right)+c_{1\varepsilon}\bar{\rho}\frac{\varepsilon}{k}(P+G)(1+c_{3\varepsilon}R_f')-c_{2\varepsilon}\bar{\rho}\frac{\varepsilon^2}{k} \tag{2}$$

where $P=-\overline{u_i'' u_j''}(\partial\tilde{u}_i/\partial x_j)$ and is modeled as $P=\upsilon_t(\partial\tilde{u}_i/\partial x_j+\partial\tilde{u}_j/\partial x_i)\partial\tilde{u}_i/\partial x_j$, R_f' is the modified flux Richardson number, $G=-\beta\overline{u_i''T''}a_{gi}$ and is modeled as $G=\beta(\upsilon_t/\sigma_t)(\partial\tilde{T}/\partial x_i)a_{gi}$, β is the thermal expansion coefficient $-(1/\bar{\rho})(\partial\bar{\rho}/\partial\tilde{T})$.

The governing equation for an ordinary scalar, such as mass fraction and enthalpy, reads

$$\frac{\partial(\bar{\rho}\tilde{\varphi})}{\partial t}+\frac{\partial(\bar{\rho}\tilde{u}_j\tilde{\varphi})}{\partial x_j}=\frac{\partial}{\partial x_j}\left(\frac{\mu}{P_r}\frac{\partial\tilde{\varphi}}{\partial x_j}-\bar{\rho}\overline{u_j''\varphi''}\right)+\bar{S}_\varphi \tag{3}$$

where $\bar{S}_\varphi$ is the source term and P_r represents the Prandtl or Schmidt number.

The numerical constants and their sources are listed in Table 1.

Due to its simplicity, this standard buoyancy-modified

Table 1
Numerical constants

Constant	c_μ	$c_{1\varepsilon}$	$c_{2\varepsilon}$	$c_{3\varepsilon}$	σ_k	σ_ε	σ_T	σ_φ	c_g
Value	0.09	1.44	1.92	0.0[a] 0.8[b]	1.0	1.3	0.7	0.7	2.0
Ref.	[13]	[13]	[13]	[13]	[13]	[13]	[14]	[14]	[14]

[a] is for vertical flow.
[b] is for horizontal flow.

k–ε model has been widely used to study buoyant diffusion flame and smoke movement in fires [2–8]. However, it is well known that this model tends to seriously under-predict the spreading rate of vertical buoyant jets [5, 6] and over-predict the entrainment of horizontal, stably-stratified flow [9]. Since the buoyancy production term, G in the k equation, is positive in unstable flow and negative in stable flow, the role of buoyancy is to amplify or damp turbulence. Therefore, the magnitude of G is likely to be under-estimated by simple gradient modeling. This is evidenced in Shabbir and Taulbee's investigation [10]. In their study of an axisymmetric plume, they found that the measured axial heat flux, $\overline{u''T''}$, was generally several times larger than that modeled in the simple gradient form, but agreed reasonably well with that modeled in the following ASM form,

$$\overline{u_i''T''} = \frac{1}{c_{1t}}\frac{k}{\varepsilon}\left(-\overline{u_i''u_j''}\frac{\partial \tilde{T}}{\partial x_j} - (1-c_{2t})\overline{u_j''T''}\frac{\partial \tilde{U}_i}{\partial x_j} - (1-c_{3t})\beta a_{gi}\overline{T''^2}\right) \quad (4)$$

where $\overline{T''^2} = -R(k/\varepsilon)\overline{u_i''T''}(\partial\tilde{T}/\partial x_i)$, c_{1t}, c_{2t}, c_{3t} and R are constants [10].

Attempts were made to adopt the above formula to model $\overline{u_i''T''}$ in this work. However, it was found difficult to reach convergence. We thus turned to the generalized gradient diffusion hypothesis of Daly and Harlow [15], which is simpler, and reads

$$\overline{u_i''T''} = -c_t\frac{k}{\varepsilon}\overline{u_i''u_j''}\frac{\partial \tilde{T}}{\partial x_j} \quad (5)$$

where $c_t = \frac{3}{2}c_\mu/\sigma_T$.

This diffusion hypothesis was probably first used by Ince and Launder [16]. As will be seen later, the magnitude of $\overline{u''T''}$ in eq. (5) is generally several times larger than that in the simple gradient modeling form. This indicates that the generalized diffusion hypothesis is more realistic.

In the ASM, the Reynolds stress is given by

$$\overline{u_i''u_j''} = \tfrac{2}{3}\delta_{ij}k + \frac{k}{\varepsilon}\frac{(1-c_2)(P_{ij}-\frac{2}{3}\delta_{ij}P)}{c_1+(P+G)/\varepsilon-1} + \frac{k}{\varepsilon}\frac{(1-c_3)(G_{ij}-\frac{2}{3}\delta_{ij}G)}{c_1+(P+G)/\varepsilon-1} \quad (6)$$

which indicates there is a direct effect of buoyancy on $\overline{u_i''u_j''}$. Although it is much simpler than the $\overline{u_i''u_j''}$ equation in the RSM, this formula is still rather complex.

In order to simplify it, Davidson [17] proposed a second closure correction method and rewrote the above expression as

$$\overline{u_i''u_j''} = \tfrac{2}{3}\delta_{ij}k + \frac{k}{\varepsilon}\frac{(1-c_2)(P_{ij}-\frac{2}{3}\delta_{ij}P)}{c_1+(P+G)/\varepsilon-1} + \frac{k}{\varepsilon} \quad (7)$$

$$\frac{(1-c_3)(G_{ij}-\frac{2}{3}\delta_{ij}G)}{c_1+(P+G)/\varepsilon-1} = (\overline{u_i''u_j''})_{k-\varepsilon} + (\overline{u_i''u_j''})_{\text{asm}}$$

where

$$P_{ij} = -\overline{u_i''u_l''}\frac{\partial \tilde{u}_i}{\partial x_l} - \overline{u_j''u_l''}\frac{\partial \tilde{u}_i}{\partial x_l},$$

$$G_{ij} = -\beta\overline{u_i''T''}a_{gj} - \beta\overline{u_j''T''}a_{gi},$$

$$(\overline{u_i''u_j''})_{\text{asm}} = \frac{k}{\varepsilon}\frac{(1-c_3)(G_{ij}-\frac{2}{3}\delta_{ij}G)}{c_1+(P+G)/\varepsilon-1},$$

$$(\overline{u_i''u_j''})_{k-\varepsilon} = \tfrac{2}{3}\delta_{ij}k + \frac{k}{\varepsilon}\frac{(1-c_2)(P_{ij}-\frac{2}{3}\delta_{ij}P)}{c_1+(P+G)/\varepsilon-1}$$

and was modeled by the formula in the standard k–ε model as

$$(\overline{u_i''u_j''}) = -\upsilon_t\left(\frac{\partial \tilde{u}_i}{\partial x_j} + \frac{\partial \tilde{u}_j}{\partial x_i}\right) + \tfrac{2}{3}k\delta_{ij}.$$

The term $(P+G)/\varepsilon-1$ in the denominator will disappear if the local equilibrium assumption is adopted.

The Reynolds stress appears in the momentum equations, the turbulence kinetic energy production term, P, and the generalized gradient modeling formula of eq. (5). The numerical experiments in this work indicated that the inclusion of $(\overline{u_i''u_j''})_{\text{asm}}$ in the momentum equations and eq. (5) will create numerical difficulty when the model is coupled with complex combustion and radiation models to study the buoyant diffusion flame. Thus, we only introduced $(\overline{u_i''u_j''})_{\text{asm}}$ into the turbulence kinetic energy shear production term P, which appears in both k and ε equations,

$$P = -\overline{u_i''u_j''}\frac{\partial \tilde{u}_i}{\partial x_j} = -[(\overline{u_i''u_j''})_{k-\varepsilon} + (\overline{u_i''u_j''})_{\text{asm}}]\frac{\partial \tilde{u}_i}{\partial x_j} \quad (8)$$

In the present model, the production term is computed as

$$P = (P)_{k-\varepsilon}(1-R_f) \quad (9)$$

where

$$(P)_{k-\varepsilon} = \upsilon_t\left(\frac{\partial \tilde{u}_i}{\partial x_j} + \frac{\partial \tilde{u}_j}{\partial x_i}\right)\frac{\partial \tilde{u}_i}{\partial x_j}.$$

In consistency with the heat flux $\overline{u_i'' T''}$ modeling, all the scalar fluxes in eq. (3) are modeled in the generalized gradient diffusion form.

All the empirical model constants keep their values from the standard k–ε model except for $c_{3\varepsilon}$, which is directly related to buoyancy effect. In the standard buoyancy-modified k–ε model, different values of $c_{3\varepsilon}$ were recommended [13], varying with flow conditions from about 0.0 to about 1.0. In the present model, we recommend a value of 0.6 for $c_{3\varepsilon}$, largely based on numerical experiments.

3. Numerical method

The control volume method was employed, with PLDS (Power Law Differential Scheme) [18]. The SIMPLE [18, 19] pressure correction algorithm was adopted. A non-uniform grid, clustered towards high gradients region, was used. The steady state solution was obtained by simulating the physical transient process for sufficient long time until steady state is reached. Numerical sensitivity computations were performed, indicating that all the numerical results presented are essentially grid-independent and radiation ray-number independent (in the diffusion flame simulation).

4. Basic test of the model

4.1. Two-dimensional plane thermal plume test

As a basic test, the modified model was first applied to a two-dimensional, plane thermal plume. A two-dimensional, plane thermal plume is often chosen as a preliminary test case for model development, since it is simple, self-similar and extensive experimental data are available for comparison.

This flow is symmetric with respect to the plume central line, and essentially parabolic, i.e., the downstream flow characteristic is mainly determined by the upstream flow. Due to its symmetry, the computation was only carried out on half of the plane with symmetric boundary condition imposed at the plume central line. The computation domain was extended to 1.0 m away from and 2.7 m above the center of the plume source exit (plume source exit half width is 0.03 m), where free and exit boundary conditions were adopted, respectively. The plume source flow was assumed to be laminar with uniform velocity and temperature. The presented results were obtained using a non-uniform grid of 50×40.

The spreading rate of a vertical thermal jet is of critical importance. The predicted spreading rates based on half central line velocity and half central line temperature increase are compared in Table 2 with experimental measurements [20]. The results of this model are promising, and agree well with experimental data.

Computation was also performed using the standard buoyancy-modified k–ε model, and the predicted spreading rates are also listed in Table 2. One can clearly see that the standard k–ε model seriously under-predicts the spreading rates of the thermal plume, by about 30%. In the k–ε model, the turbulent transport is closely related to the turbulent transport coefficient, which is proportional to c_μ and inversely proportional to the turbulent Prandtl number σ_φ. As expected, a larger value of c_μ and a smaller value of σ_φ will result in increased spreading rates. One may be able to fit specific experimental data by simply adjusting the constants c_μ and σ_φ, as Nam and Bill have done [6]. However, it is not reasonable to adjust the standard constants arbitrarily without any fundamental basis, otherwise the generality of the turbulence model will be lost.

Figure 1 shows the computed and measured velocity and temperature profiles. As shown in the figure, the profiles predicted by this model match experimental measurements very well.

Figure 2 presents the computed turbulence kinetic energy profiles. For reference, it is compared with that of Hossain and Rodi's ASM study [21]. There is reasonably good agreement between these two computations, although there are some difference. This model predicted a higher turbulence kinetic energy at the central line. The difference in the buoyancy production rates of the turbulence kinetic energy given by the two different mod-

Table 2
Comparison of spreading rates

Source	Experiment [20]	Present model	Standard k–ε
$dy_{0.5U}/dx$	0.120	0.120	0.081
$dy_{0.5T}/dx$	0.130	0.123	0.080

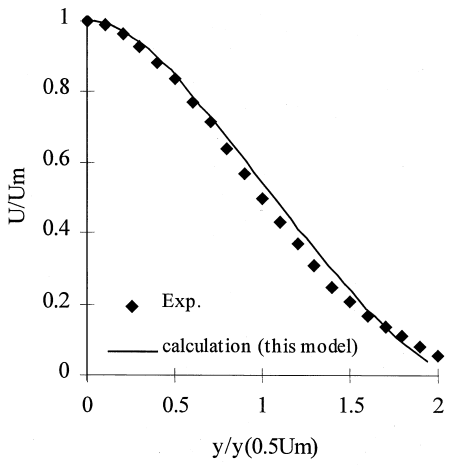

a). U / U_m vs $y / y_{0.5U_m}$

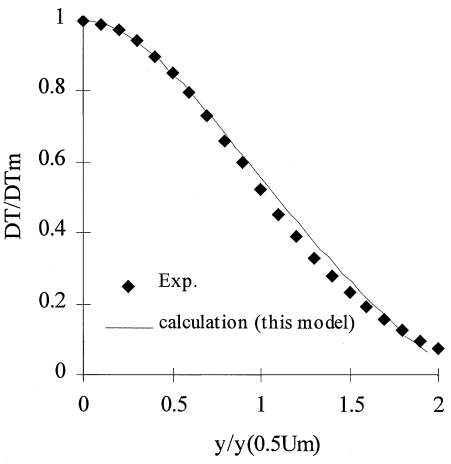

b). $\Delta T / \Delta T_m$ vs $y / y_{0.5U_m}$

Fig. 1. Comparison of velocity and temperature profiles (a) U/U_m vs $y/y_{0.5U_m}$, (b) $\Delta T/\Delta T_m$ vs $y/y_{0.5U_m}$.

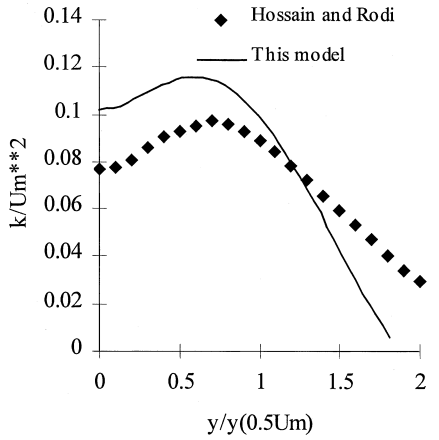

Fig. 2. k/U^2_m vs $y/y_{0.5U_m}$.

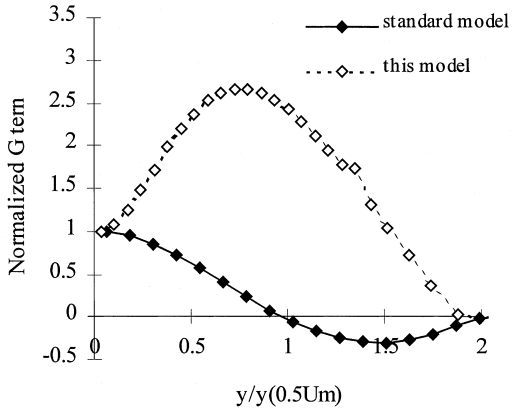

Fig. 3. Variation of buoyancy production rate, G, normalized by its central line value. Note: in this and later figures, standard model = the standard buoyancy-modified k–ε model.

els is probably one of the main reasons. At the central line, G is zero in Hossain and Rodi's ASM study [21], while a positive value was obtained with this model. As shown in [10], experimental measurement of an axisymmetric thermal plume indicated a positive value of G at the central line. Another difference is that the turbulence kinetic energy decreases faster toward the plume edge in the present model.

Figure 3 clearly shows that the G term given by generalized gradient modeling is generally much larger than that by simple gradient modeling. At the plume edge, where $y/y_{0.5U_m}$ is about 1.5 and the vertical component of the temperature gradient is negative, simple gradient modeling gives a negative value of G, which is of the opposite sign to that given by generalized gradient modeling. This implies that the counter gradient diffusion is accounted for by generalized gradient modeling. Considering Shabbir and Taulbee's finding concerning the axial heat flux $\overline{u''T''}$ [10], Fig. 3 indicates that it is important to replace simple gradient modeling of scalar fluxes at least by generalized gradient modeling.

4.2. Axisymmetric thermal plume test

Since some previous turbulence models tuned to plane flow turn out to fail in axisymmetric situations [13], this further test was carried to verify that the present model is free from this weakness.

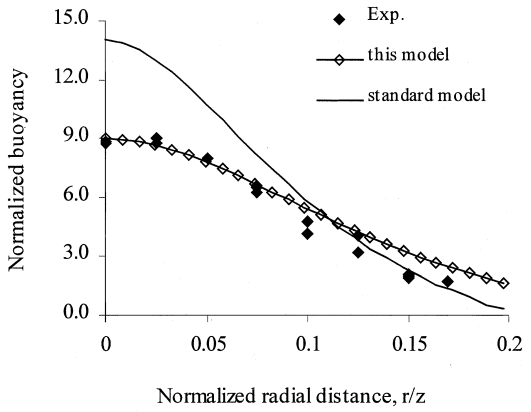

Fig. 4. Normalized buoyancy profile.

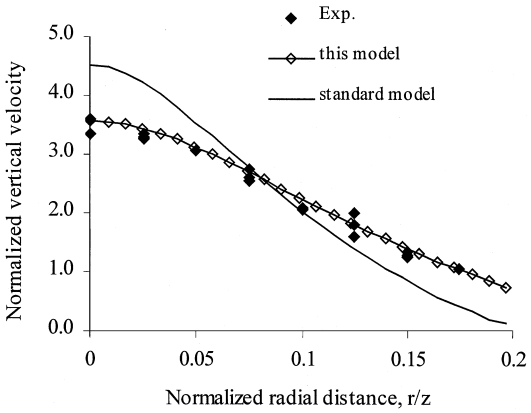

Fig. 5. Normalized vertical velocity profile.

The experiment conducted by George et al. [22] was simulated, using both the present model and the standard buoyancy-modified k–ε model. The computation domain was extended to 0.9 m away from (radial direction) and 3.5 m above the center of the plume source exit. The boundary conditions are similar to those used in the plane plume case, but the flow is now axisymmetric. A non-uniform grid of 40×40 was employed.

Figures 4 and 5 show the predicted and measured normalized velocity and buoyancy profiles. The normalized vertical velocity and buoyancy are defined as: $v(z/F_0)^{1/3}$ and $|a_{gi}|(\Delta\rho/\rho_\infty)(z^5/F^2_0)^{1/3}$, where v is the vertical velocity, z is the height above the virtual origin of the plume and F_0 is the buoyancy parameter. In this particular problem, the virtual origin of the plume was found to be in the plane of the plume source exit and F_0 is 1.0×1.0^6 cm^4/s^3 [22]. It can be seen that the predictions by the present model agree very well with measurements and are much better than those by the standard buoyancy-modified k–ε model.

5. Application to a buoyant diffusion flame

In order to verify the applicability of the developed turbulence model to the simulation of fires, the model was coupled with complex combustion and radiation models to study a buoyant diffusion flame. The results are compared with those of standard buoyancy modified k–ε model and the measurement. This application is also a further validation of the developed turbulence model.

In this particular application, the flamelet concept [23–25] was employed to study combustion. With the radiation properties of the combustion products, including soot, water vapor and carbon dioxide, presented by Modak's curve fit method [26], the discrete transfer method [27] was used to calculate the radiation.

5.1. The combustion model

Combustion was considered using the flamelet concept [23–25] which is based on the mixing control assumption. In the flamelet concept, the turbulent flame is considered to be an ensemble of wrinkled laminar flamelets which have a well-defined structure. The instantaneous chemical species concentration is simply related to the local value of the mixture fraction. Chemistry turbulence interactions are included by treating the turbulent reacting flow as a random process and introducing a probability density function (pdf). The following two equations are solved for a conserved scalar (mixture fraction) and the variance of mixture fraction, respectively,

$$\frac{\partial(\bar{\rho}\tilde{f})}{\partial t}+\frac{\partial(\bar{\rho}\tilde{u}_j\tilde{f})}{\partial x_j}=\frac{\partial}{\partial x_j}\left(\frac{\mu}{S_c}\frac{\partial\tilde{f}}{\partial x_j}-\bar{\rho}\overline{u_j''f''}\right) \tag{10}$$

$$\frac{\partial(\bar{\rho}\tilde{g})}{\partial t}+\frac{\partial(\bar{\rho}\tilde{u}_j\tilde{g})}{\partial x_j}=\frac{\partial}{\partial x_j}\left(\frac{\mu}{S_c}\frac{\partial\tilde{g}}{\partial x_j}-\bar{\rho}\overline{u_j''g}\right)-2\bar{\rho}\overline{u_j''f''}\frac{\partial\tilde{f}}{\partial x_j}-c_g\bar{\rho}\tilde{g}\frac{\varepsilon}{k} \tag{11}$$

where the mixture fraction is defined as

$$f=\frac{(Y_F-Y_O/s)_{\text{mixture}}-(Y_F-Y_O/s)_{\text{oxidant}}}{(Y_F-Y_O/s)_{\text{fuel}}-(Y_F-Y_O/s)_{\text{oxidant}}},$$

(Y_F-Y_O/s) is the Shvab–Zeldovich variable, s represents the stoichiometric ratio, and g is the variance of the mixture fraction f''^2.

The prescribed pdf is then constructed using the mixture fraction and its variance. In this study, the normalized Beta function [25] was adopted.

5.2. Soot modeling

Sooting is a complex phenomenon which includes soot formation and oxidation. Soot is mainly formed in the fuel rich region of the flame through a complex chemical

process converting gas fuel of few carbon atoms to a solid particle which contains up to a million carbon atoms, and exhibits no unique chemical or physical structure. This process comprises nucleation, coagulation and surface growth. The formed soot can be oxidized by O_2 and the OH radical when transported to the lean region. Although some progress has been made in soot modeling [28] in recent years, turbulent soot modeling is still in its infancy. In this study, soot was approximately considered by assuming that a certain proportion of the parent fuel was converted to soot. The conversion factor, 10%, was taken from the literature [29].

5.3. The radiation model

In this study, the discrete transfer (DT) method [27] was adopted to calculate the radiation. Modak's curve-fit method [26] was incorporated to predict the radiation properties of the combustion products. Since the radiation is highly nonlinear, the consideration of the influence of turbulent fluctuation on radiation is clearly desirable. However, the computational complexity and the computer capacity required will be greatly increased. As an approximation, the radiation was computed using mean scalars in this study.

In the discrete transfer method, the radiation equation, with the following form, is solved along a discrete set of directions (rays) from every element of the boundary surface,

$$\frac{\partial I_{w,l}}{\partial l} = -\zeta_{w,l} I_{w,l} + \zeta_{w,l} I^0_{w,l} \tag{12}$$

where the superscript 0 denotes black-body and w the wavenumber.

5.4. Brief description of the simulated flame

The simulated experiment was conducted by Andersson et al. [30]. In this experiment, a circular burner was placed at the center of a open-top cylinder which is 3 m in diameter and 2 m in height. The diameter of the burner was 90 mm and the fuel (C_3H_6) supply rate 0.28 g/s. In order to obtain a stable axisymmetric flame, air was introduced through the floor of the cylinder at a velocity of 0.3 m/s.

5.5. Results and discussion

The numerical simulations were carried out using both the standard buoyancy-modified turbulence model and the present model. In the simulations, the flame was assumed ideally axisymmetric. The computations considered the whole space inside the cylinder, but took full advantage of the axisymmetry. The burner exit flow was assumed laminar and uniform. At solid surfaces, non-slip wall boundary condition was employed. A non-uniform grid of 50×46 was used.

The predicted profiles were compared with experimental measurements. In order to show the symmetry of the experimental flame, most of the profiles are plotted on both sides of the burner.

Figure 6(a)–(k) show the predicted and measured velocity, temperature and composition profiles at three different heights: 0.9, 1.2 and 1.5 m above the burner. These figures clearly show that the width of the thermal plume predicted by the standard buoyancy-modified k–ε model is much narrower than both measurements and the prediction of the present model. Using the standard buoyancy-modified k–ε model, the velocity, temperature and concentration of combustion products at the plume center are all significantly over-predicted. Correspondingly, the concentration of oxygen at the plume center is severely under-predicted. This is consistent with the findings in some earlier studies [5, 6]. The main reason is that turbulent transport is seriously under-predicted by the standard buoyancy-modified k–ε model, as indicated in the model test section. The results given by the present model are in a close agreement with measurements. The spreading rates, plume width, and the velocity, temperature and composition profiles are all reproduced quite well using the present model. The difference in central line values between measurements and the predictions of the present model is within about 10%. Due to the crudeness of the soot modeling and the large uncertainty in the experimental measurement of soot volume fraction [30] (up to a factor of 3), there is a considerable difference between the predicted and measured soot volume fraction profiles.

Figures 7 and 8 show the predicted and measured decay of the velocity and temperature fields along the central line of the fire plume. Both figures indicate that the predictions of the present model fit experimental data quite well, while there is a significant difference between the predictions of the standard buoyancy-modified model and experimental data. From Fig. 8, one may deduce that the flame predicted by the standard buoyancy-modified k–ε model is likely to be much narrower and longer than in reality, while the flame shape predicted by the present model is much more realistic.

As one would expect, the decay of the temperature field is much faster than that of the velocity field, which decreases slowly along the central line, due to the acceleration by buoyancy. The self-similar structure of the pure axisymmetric thermal plume indicates that $\Delta T_m \propto x^{-5/3}$ and $U_m \propto x^{-1/3}$. Due to the involvement of combustion and radiation, the decay of the velocity and thermal fields in this study is somewhat different from that of a pure thermal plume. But the general trend is still valid here, i.e., the temperature field decays much faster than the velocity field.

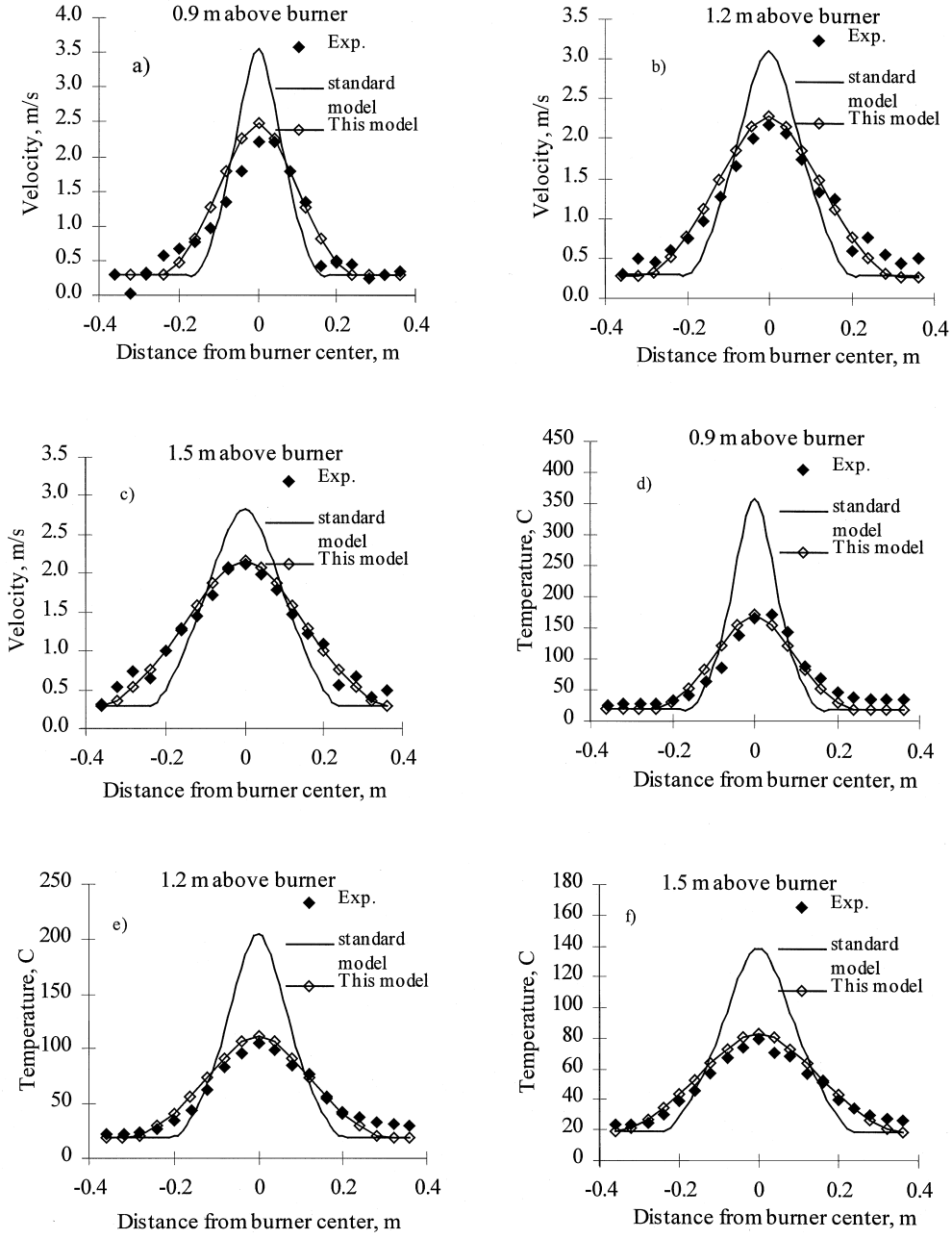

Fig. 6. Velocity, temperature and composition profiles at three different heights above the burner: 0.9, 1.2 and 1.5 m.

6. Conclusions

A modified k–ε two-equation model has been developed to improve the consideration of the important buoyancy effect on turbulence and turbulent transport. The present model was tested against both plane and axisymmetric thermal plumes, and a buoyant diffusion flame which represents fires. The predictions agree well with both experimental measurements and Hossain and Rodi's study of the thermal plume. When compared with the standard buoyancy-modified k–ε model, this model constitutes a significant improvement in prediction accuracy.

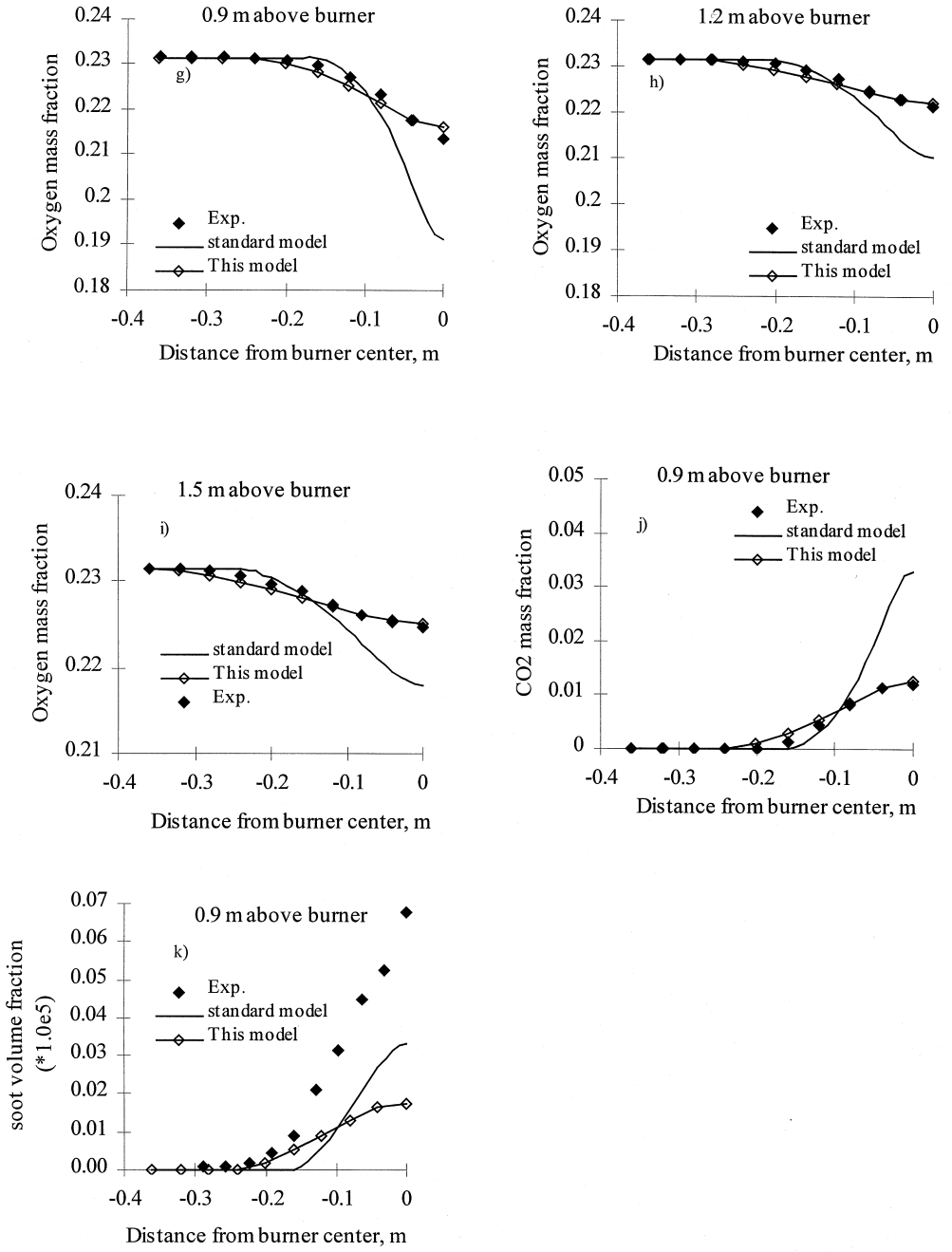

Fig. 6. *Continued.*

The model was found to be stable, computationally economic, promising and applicable to complex situations. It can be easily incorporated into the widely used k–ε based CFD codes. This would be useful in the numerical prediction of a buoyant flame and flow.

Since this model is still k–ε based, many disadvantages of the k–ε type of models remain. For example, its applicability to the flow of strong rotation or streamline curvature can be limited. Further research is necessary to refine this preliminary work.

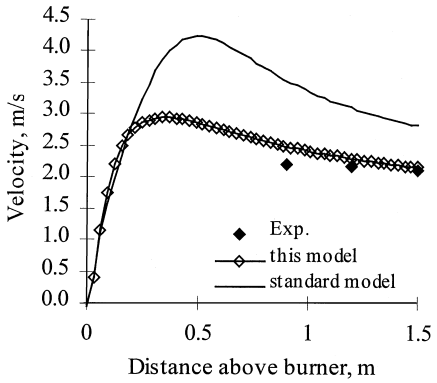

Fig. 7. Central line velocity.

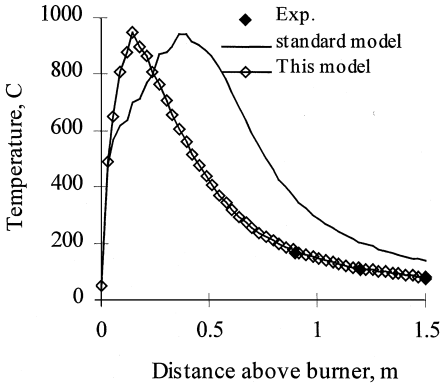

Fig. 8. Central line temperature.

References

[1] D.C. Wlicox, Turbulence modeling for CFD, DCW Industries, 1993.

[2] N.C. Markatos, M.R. Malin, G. Cox, Mathematical modeling of buoyancy-induced smoke flow in enclosures, Int. J. Heat Mass Transfer 25 (1982) 63–75.

[3] S. Kumar, G. Cox, Mathematical modeling of fires in road tunnels, Fifth International Symposium on the Aerodynamics and Ventilation of Vehicle Tunnels, 1985, pp. 61–76.

[4] G. Cox, S. Kumar, Field modeling of fire in forced ventilated enclosures, Combust. Sci. Technol. 52 (1987) 7–23.

[5] M.O. Annarumma, J.M. Most, P. Joulain, On the numerical modeling of buoyant-dominated turbulent vertical diffusion flames, Combustion and Flame 85 (1991) 403–415.

[6] S. Nam, R.G. Bill, Numerical simulation of thermal plumes, Fire Safety Journal 21 (1993) 231–256.

[7] Z. Yan, G. Holmstedt, CFD and experimental studies of room fire growth on wall lining materials, Fire Safety Journal 27 (1996) 201–238.

[8] Z. Yan, G. Holmstedt, CFD simulation of upward flame spread over fuel surface, Fifth Int. Symp. on Fire Safety Science, Australia, 1997.

[9] P. Woodburn, Computational fluid dynamics simulation of fire-generated flows in tunnels and corridors, Ph.D. Thesis, University of Cambridge, 1995.

[10] A. Shabbir, D.B. Taulbee, Evaluation of turbulence models for predicting buoyant flows, Journal of Heat Transfer 112 (1990) 945–951.

[11] P.G. Huang, M.A. Leschziner, Stabilization of recirculating-flow computations performed with second-moment closures and third-order discretization, Proceedings of Fifth Int. Symp. on Turbulent Shear Flows, Cornell, 1985, pp. 20.7–20.12.

[12] M.A. Leschziner, Numerical implementation and performance of Reynolds-stress closures in finite-volume computations of recirculating and strongly swirling flows, Lecture notes to Introduction to the Modeling of Turbulence, von Karman Institute for Fluid Dynamics, 1987.

[13] W. Rodi, Turbulence models and their application in hydraulics: a state of the art review, SBF Report 80/T/125, University of Karlsruhe, 1980.

[14] G. Cox, Compartment fire modeling, in: G. Cox (Ed.), Combustion Fundamentals of Fire, chap. 6, Academic Press, 1995.

[15] B.J. Daly, F.H. Harlow, Transport equations of turbulence, Physics Fluids 13 (1970) 2634–2649.

[16] N.Z. Ince, B.E. Launder, On the computation of buoyancy-driven turbulent flows in rectangular cavites, Proc. 2nd UK national Conf. On Heat Transfer, Univ. of Strathclyde, Glasgow, vol. 2, 1988, pp. 1389–1400.

[17] L. Davidson, Second-order correction of the k–ε model to account for non-isotropic effects due to buoyancy, Int. J. Heat Mass Transfer 33 (1990) 2599–2608.

[18] S.V. Patankar, Numerical Heat Transfer and Fluid Flow, Hemisphere, New York, 1980.

[19] S.V. Patankar, D.B. Spalding, A calculation procedure for heat, mass and momentum transfer in three-dimensional parabolic flows, Int. J. Heat Mass Transfer 15 (1972) 1787–1806.

[20] J.C. Chen, W. Rodi, Turbulent Buoyant Jets: a Review of Experimental Data, HMT, vol. 4, Pergamon, 1980.

[21] M.S. Hossain, W. Rodi, A turbulence model for buoyant flows and its application to vertical buoyant jet, in: W. Rodi (Ed.), Turbulent Buoyant Jets and Plumes, Pergamon, New York, 1982, pp. 121–178.

[22] W.K. George, R.L. Alpert, F. Tamanini, Turbulence measurements in an axisymmetric buoyant plume, Int. J. Heat Mass Transfer 20 (1977) 1145–1154.

[23] N. Peters, Laminar flamelet concepts in turbulent combustion, Twenty-first Symp. (International) on Combustion, The Combustion Institute, Pittsburgh, 1986, pp. 1231–1250.

[24] N. Peters, Laminar diffusion flamelet models in non-premixed turbulent combustion, Prog. Energy Combust. Sci. 10 (1984) 319.

[25] S.K. Liew, K.N.C. Bray, J.B. Moss, A stretched laminar flamelet model of turbulent nonpremixed combustion, Combustion and Flame 56 (1984) 199–213.

[26] A.T. Modak, Radiation from products of combustion, Fire Research 1 (1978) 339–361.

[27] F.C. Lockwood, N.G. Shah, A new radiation solution method for incorporation in general combustion prediction procedures, Eighteenth Symp. (Int.) on Combustion, The Combustion Institute, Pittsburgh, 1981, pp. 1405–1414.

[28] H. Bockhorn, in: H. Bockhorn (Ed.), Soot Formation in Combustion: Mechanisms and Models, Springer, 1994.
[29] A. Tewarson, Generation of heat and chemical compounds in fires, in: P.J. DiNenno et al. (Eds.), The SFPE Handbook of Fire protection Engineering Second Edition, 1995, pp. 3.53–3.124.
[30] P. Andersson, Assessment and mitigation of industrial fire hazards, PhD. Thesis, Lund University, 1997.